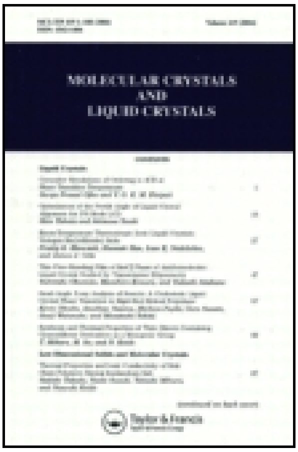

Molecular Crystals and Liquid Crystals Science and Technology. Section A. Molecular Crystals and Liquid Crystals
Publication details, including instructions for authors and subscription information:
http://www.tandfonline.com/loi/gmcl19

New LMM Organosiloxanes with Photoisomerising AZO Groups

Joanna Newton [a] [b] , Harry Walton [a] , Harry Colest [a] & Philip Hodges [b]
[a] Liquid Crystal Group, Department of Physics and Astronomy, University of Manchester, Manchester, M13 9PL, England
[b] Polymer Synthesis Group, Department of Chemistry, University of Manchester, Manchester, M13 9PL, England

To cite this article: Joanna Newton , Harry Walton , Harry Colest & Philip Hodges (1995): New LMM Organosiloxanes with Photoisomerising AZO Groups, Molecular Crystals and Liquid Crystals Science and Technology. Section A. Molecular Crystals and Liquid Crystals, 260:1, 107-125

To link to this article: http://dx.doi.org/10.1080/10587259508038686

Mol. Cryst. Liq. Cryst. 1995, Vol. 260, pp. 107–125
Reprints available directly from the publisher
Photocopying permitted by license only

NEW LMM ORGANOSILOXANES WITH PHOTOISOMERISING AZO GROUPS

JOANNA NEWTON†‡, HARRY WALTON†, HARRY COLES†*
AND PHILIP HODGE‡

† Liquid Crystal Group, Department of Physics and Astronomy and ‡ Polymer Synthesis Group, Department of Chemistry, University of Manchester, Manchester M13 9PL, England.

* Author for correspondence

Abstract A new LMM photo-reactive chiral azo-containing organosiloxane ($C_{10}Azo^{*}B$) and its racemic analogue ($C_{10}Azo^{(\pm)}B$) have been synthesised and their mesomorphic properties investigated. The materials are denoted $C_{10}Azo^{*}B$ and $C_{10}Azo^{(\pm)}B$ where C_n refers to the number of methylene units in the alkyl spacer, Azo^{*} and $Azo^{(\pm)}$ denote the chiral and racemic photoisomerising azobenzene-based mesogenic moiety and B refers to the pentamethyldisiloxane tail. Both LMM siloxane derivatives exhibit a single enantiotropic smectic A phase. Results on the consequences of incorporating these new materials into a related fast switching, LMM ferroelectric organosiloxane host will be given. In addition results will be presented on the photoisomerisation of the azo materials and their use in optically manipulating the magnitude of spontaneous polarisation in a ferroelectric liquid crystal.

INTRODUCTION

Much of the research carried out to date into the development of liquid crystals for possible device applications has utilised the ability of liquid crystals to alter the properties of light reflected from, or transmitted through, them. The ease with which molecular ordering, described in terms of an order parameter S, and hence the optical properties of liquid crystals can be altered by the application of electric fields makes them good candidates for use in electro-optic displays. Recently however interest has grown in photomechanical effects in which it is the incident light itself, rather than applied electric fields, which triggers molecular re-ordering in a liquid crystal system[1-5]

Photomechanical molecular reordering processes can be achieved by the incorporation of photoisomerising molecules into an anisotropic system. This can be achieved either by doping a host liquid crystal system with some guest photoisomerising agent, or by chemical fixation of an isomerising unit directly onto the liquid crystal molecules (as side chain moieties in a polymer system for example). Illumination with light of the correctly chosen wavelength induces isomerisation and since the bulk properties of a liquid crystal depend intimately upon microscopic steric and electrostatic interactions, the forces resulting from small changes in these molecular properties can be magnified to produce dramatic changes in macroscopic continuum quantities.

With the aim of continuing our investigation of photomechanical effects in liquid crystals we have synthesised a new low molar mass (LMM) organosiloxane, containing a photoisomerising azo group. These organosiloxane materials have excellent properties for use in electro-optic devices as they combine the ruggedness of polymer systems with the lower viscosities and response times of conventional LMM systems[6]. The direct incorporation of a photoisomerising azo unit into the organosiloxane liquid crystal was carried out in order to limit the problems of immiscibility of an organic azo guest dye with the organosiloxane host liquid crystal, and to reduce problems of phase separation that might occur during isomerisation[3].

Azo dyes have attracted considerable interest as photoisomerising molecules both for the reversibility of, and the large steric change involved in, the isomerisation process (shown schematically in Figure 1). Several Groups [4,5] have demonstrated the ability of photo-reactive azo molecules dissolved in a liquid crystal nematic host, to induce an isothermal transition to the isotropic state upon UV irradiation of the *trans* azo molecules, resulting in their transition to the *cis* state. It is assumed that the bent *cis* isomer packs less easily into the nematic matrix than the more linear *trans* isomer, and tends to disrupt the packing of the liquid crystal molecules. If a sufficiently large population of *cis* isomers is created by UV illumination, the system is eventually driven into the isotropic state.

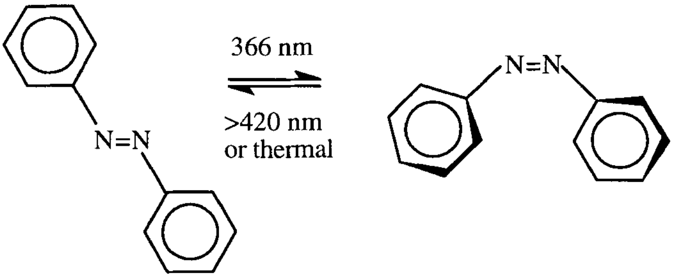

FIGURE 1 *Trans-cis* isomerisation of azobenzene

Recently we have extended study of photomechanical effects to investigate the smectic phases of liquid crystals[1-3]. In particular we have investigated photomechanical effects in the (ferroelectric) chiral smectic C (S_C^*) phase of various liquid crystals. Since the prediction[7] of ferroelectricity in the S_C^* phase, significant technological interest has arisen around this phase due to the possibility of using ferroelectric liquid crystals to construct fast (μs) optical switches for use in high information content displays and optical data storage devices. A particularly attractive feature of such systems is that molecules can be made to switch between two stable tilted positions by the application of an electric field[8]. Our studies have shown that by doping a S_C* material (SCE13, Merck) with low concentrations (<10% wt:wt) of a mesomorphic azo dye (denoted N5, Figure 2), it is possible to alter isothermally the bulk properties of the system on illumination by low power density UV light (360 nm, <10mWcm^{-2}) . Upon such illumination and subsequent conversion of the azo dye to its bent *cis* isomer, the magnitude of ferroelectric spontaneous polarisation (P_s) in the S_C^* phase of the guest host system was seen to fall, consistent with the assumption that the bent *cis* N5 molecules tend to disrupt the packing of the host liquid crystal molecules[2,3].

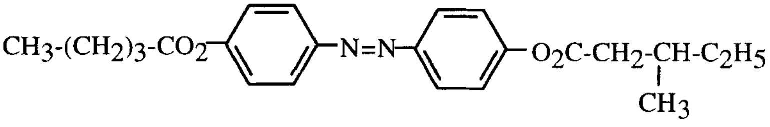

FIGURE 2 Structure of the photoisomerising dye N5

The fall in the magnitude of P_s is fully reversible upon removal of the UV light, which allows the azo molecules to relax back to their thermally favoured *trans* state. The ability to photonically alter P_s and electro-optic switching behaviour in a reversible and isothermal manner, using commercial ferroelectric mixtures with performance optimised for room temperature has implications for the development of new optical data storage devices and photonic transducers[1-3]. In order to improve the responsiveness of a system to a given power density of UV light however, it is desirable to increase the concentration of photoisomerising molecules. With the types of guest/host system we have previously employed however, increasing the concentration of guest above ~10% (wt:wt) can begin to create problems with phase separation of the azo guest dye within the liquid crystalline host and it was for this reason that we have begun to investigate the possibilities for direct chemical fixation of photoisomerising azo units into liquid crystalline molecules. In this paper we describe the synthesis and characterisation of a novel photoisomerising chiral organosiloxane and its racemic analogue and present data on the optical manipulation of spontaneous polarisation in a ferroelectric liquid crystal.

MATERIALS

In an attempt to achieve a compromise between the advantages offered by side chain liquid crystal polymer (SCLCP) systems with their increased phase stability and improved mechanical properties, and the disadvantages of the concomitant increase in the viscosity of the system, we have recently synthesised and studied a number of ferroelectric LMM organosiloxane mesogenic compounds which exhibit a room temperature S_C^* mesophase[6,9]. Materials have been prepared of the AB type where A refers to the mesogenic unit and B refers to a dimethylsiloxane end chain or spacer. We have begun to develop a good understanding of structure-property correlations in such materials[9]. A typical example of an organosiloxane material is shown in Figure 3. This material will be discussed in greater detail in later sections of this paper.

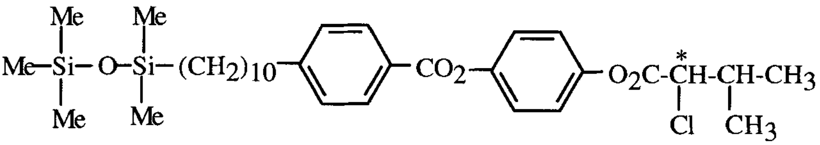

I 56.2 °C S_C^* ≈ - 4.2 °C K

FIGURE 3 Structure of $C_{10}C^*B$ with phase transition temperatures.

Although the bulky, highly flexible disiloxane tail causes a reduction in the interchain interactions and the degree of crystallinity of the alkene precursor it does not destroy the liquid-crystallinity of these AB materials. These ferroelectric LMM organosiloxane mesogens show subzero crystallisation, fast switching times and both moderate and high spontaneous polarisation with high temperature-independent tilt angles. They also appear to have well defined layer structures similar to SCLCP's[10].

The aim of the present work was to prepare a new LMM organosiloxane with a photo-reactive azobenzene group chemically incorporated into the compound. This new class of LMM organosiloxanes tends to prefer to form smectic rather than nematic phases[11]. Following X-ray studies[10] we attribute this behaviour to the microscopic aggregation of the siloxane groups into siloxane rich layers, thereby promoting a smectic layered structure. The siloxane layers appear to act almost as a polymer backbone running through the system and this confers ruggedness on the sample. The presence of branching aliphatic chains in smectogenic molecules generally favours molecular tilting within smectic layers[12] and the shortness of the azobenzene aromatic cores promotes a low viscosity[13], which is an important property for device applications.

This paper presents the synthesis and characterisation of a new LMM chiral organosiloxane containing a photoisomerising group azo (N=N) and its racemic analogue. The general structure of the materials studied is shown below in Figure 4. The materials are denoted $C_{10}Azo^{*}B$ and $C_{10}Azo^{(\pm)}B$, where C_n denotes the methylene spacer, Azo* denotes the chiral mesogenic end group and $Azo^{(\pm)}$ its racemic analogue and B denotes the pentamethyldisiloxane tail.

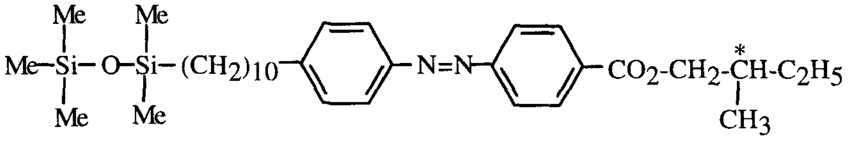

FIGURE 4 Structure of $C_{10}Azo^{*}B$ the synthetic route of which is described in this paper.

SYNTHESIS

The LMM chiral and racemic organosiloxanes were synthesised according to the general procedure outlined in Scheme 1. As a typical example, the synthesis of the $C_{10}Azo^{*}B$ derivative is reported in detail:

1.1 (*S*)-4-(2-Methylbutyloxycarbonyl)nitrobenzene

4-Nitrobenzoyl chloride (20.9 g, 0.113 mol) and (*S*)-2-methylbutanol (10 g, 0.113 mol) were dissolved in dry THF (70 ml) and then cooled down to 0 °C. A solution of pyridine, (distilled over calcium hydride) (9.4 g, 0.118 mol) in dry THF (20 ml) was added carefully dropwise. The reaction mixture was heated at reflux overnight. On cooling, the pyridinium salt was filtered off and the solvent was removed under reduced pressure. The remaining precipitate was removed using column chromatography (silica gel stationary phase) using CH_2Cl_2 as eluent. The resulting liquid was dried under vacuum at 40 °C for 24 hours. This gave the title compound as a yellow liquid. Yield = 24.45 g, 0.103 mol, (92%), CI m/z 236 (M^+), $[\alpha]^{25}_{D}$+ 6.2° (1.3 mol l^{-1}, $CHCl_3$).

^1H NMR ($CDCl_3$): δ / ppm 0.9-0.92 (t, 3H, CH_2-$C\underline{H}_3$), 0.95-0.98 (s, 3H, CH-$C\underline{H}_3$), 1.4-1.6 (m, 2H, $C\underline{H}_2CH_3$), 1.7-2.0 (m, 1H, $C\underline{H}$-CH_3), 4.2 (m, 2H, -$CO_2C\underline{H}_2$), 7.2 (m, 2H, aromatics), 8.2-8.4 (m, 2H, aromatics). IR υ / cm^{-1} : 1720 (C=O, ester) , 1530 (C-NO_2), 1275 (CO_2-CH_2CH).

Elemental analysis: Calc. C-60.75, H-6.4, N-5.9, found C-61.2, H-6.5, N-5.6.

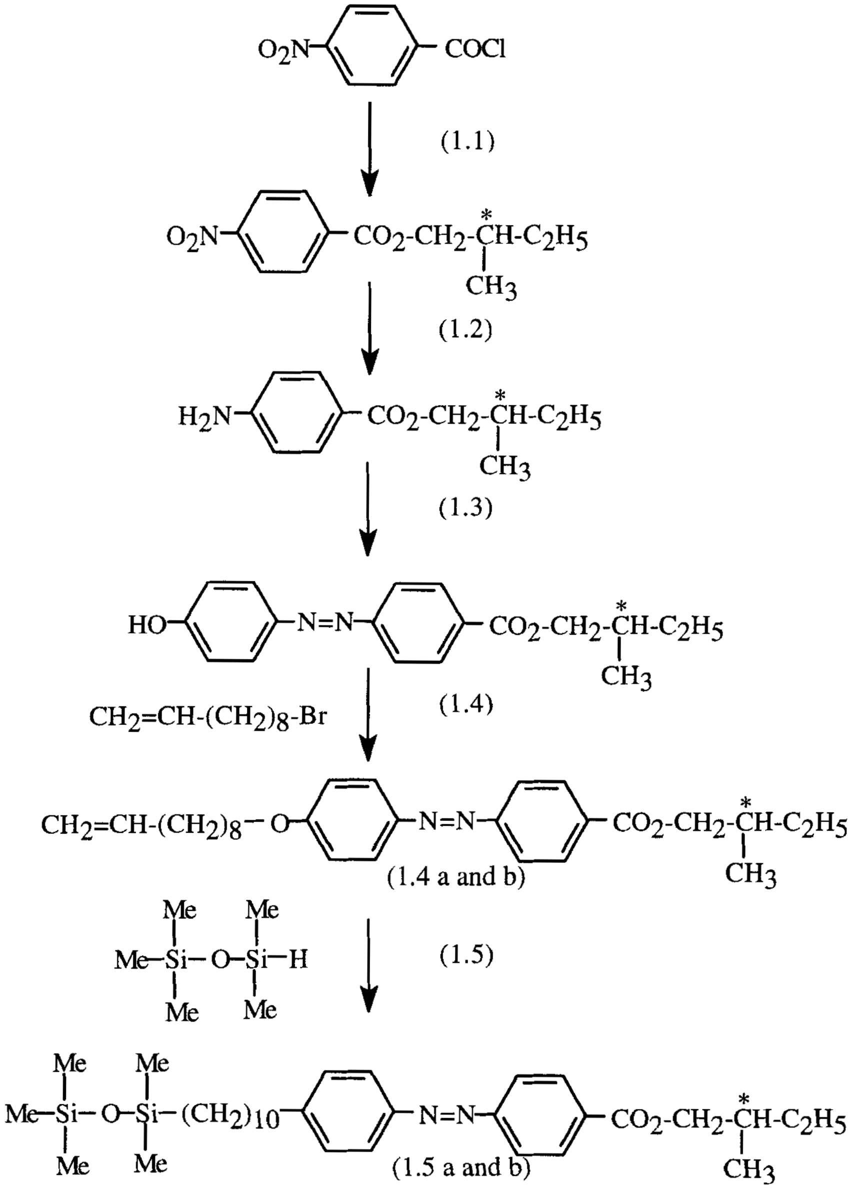

SCHEME 1

General Notes:

(1.1) C_2H_5-$CH^*(CH_3)$-CH_2-OH (or racemate), Pyridine, THF

(1.2) H_2, Pd /C (10%), EtOH

(1.3) (a) $NaNO_2$, HCl, H_2O, (b) C_6H_5OH, NaOH

(1.4) K_2CO_3, KI, MEK

(1.5) Pt^{2*}, toluene

1.2 (*S*)-4-(2-Methylbutyloxycarbonyl)aminobenzene

(*S*)-4-(2-Methylbutyloxycarbonyl)aminobenzene was prepared according to standard procedures[14]. The residue was purified by column chromatography (silica gel stationary phase) using CH_2Cl_2 as eluent. Solvent was removed under reduced pressure and the product was dried under vacuum at 40 °C for 24 hours. This gave the title compound as off-white crystals. It had m.p. 43.3-45.0 °C. Yield = 4.75 g, 0.023 mol, (89%), CI m/z 206, 205 (M^+), $[\alpha]^{25}_{D}$ + 8.4 ° (1.2 mol l^{-1}, $CHCl_3$).

^1H NMR ($CDCl_3$): δ / ppm 0.89-0.92 (t, 3H, CH_2-C$\underline{H}_3$, J = 2Hz), 0.95-0.98 (s, 2H, CH-C$\underline{H}_3$, J = 2Hz), 1.19-1.25 (m, 2H, C$\underline{H}_2$-CH_3 J = 2Hz), 1.45-1.53 (sept., 1H, C$\underline{H}$-CH_3, J = 2Hz, 3Hz), 1.76-1.84 (oct., 1H, C$\underline{H}$-CH_3, J = 2Hz), 4.02-4.06 (dd, 2H, -CO_2C$\underline{H}_2$CH-CH_3, J = 4Hz), 4.10-4.12 (d, 2H, H_2N-, J = 4Hz), 6.6 (d, 2Hz, aromatics), 7.8 (d, 2H, aromatics). IR υ / cm^{-1} : 3335 (NH_2), 1700 (C=O, ester), 1270 (CO_2CH_2).

Elemental analysis: Calc. C-69.55, H-8.3, N-6.75. found C-69.9, H-8.5 N-6.8.

1.3 (*S*)-4-Hydroxy 4'-(2-methylbutyloxycarbonyl)azobenzene

(*S*)-4-(2-Methylbutyloxycarbonyl)aminobenzene (5 g, 0.0212 mol) was dissolved in a solution of concentrated sulphuric acid (2.7 ml) and water (3 ml). The solution was cooled down to below 5 °C with constant stirring. A solution of sodium nitrite (1.56 g 0.0226 mol) in water (7 ml) was added dropwise over about 1 hour ensuring the temperature did not exceed 5 °C. The diazonium salt was then added dropwise very slowly over 1-2 hours to a solution of phenol (2.13 g, 0.0226 mol) in sodium hydroxide (10%, 12 ml), with constant stirring. After the addition was complete the solution was stirred for a further 30 minutes. The precipitate was filtered and washed with large amounts of water. The residue was purified by column chromatography (silica gel stationary phase) using hexane: ethyl acetate (3:2) as eluent. This gave the product as an orange solid. It had m.p. 114.5-116.0 °C. Yield = 5.18 g, 0.0166 mol, (74%), CI m/z 312, 311 (M^+), $[\alpha]^{25}_{D}$ +6.7 ° (1.0 mol l^{-1}, $CHCl_3$).

^1H NMR ($CDCl_3$): δ / ppm 0.6–0.8 (d, 3H, CH_2-C$\underline{H}_3$, J = 3.5Hz), 0.9-1.1 (t, 3H, CH-C$\underline{H}_3$, J = 3Hz), 1.2-1.6 (m, 2H, C$\underline{H}_2$-CH_3, J = 3Hz), 1.65-1.8 (m, 1H, CH-CH_3, J = 3Hz), 4.12-4.17 (t, 2H, -CO_2C$\underline{H}_2$CH, J = 10.5 and 7 Hz), 4.22-4.25 (m, 1H, OH, J = 9.5 and 7.5 Hz), 6.8-7.0 (d, 2H, aromatics), 7.88-7.92 (dd, 4H, aromatics), 8.12-8.16 (d, 2H, aromatics). IR υ / cm^{-1} : 3390 (O-H), 1715 (C=O, ester), 1460 and 1435 (N=N), 1280 and 1010 (CO_2OCH_2).

Elemental analysis: Calc. C-69.2, H-6.45, N-9.0, found C-69.7, H-6.80 N-9.1.

1.4 (*S*)-4-(9-Decenyloxy)-4'-(2-methylbutyloxycarbonyl)azobenzene ($C_{10}Azo^*$)

10-Bromo-1-decene (2.83 g, 0.013 mol) was added dropwise to a stirred solution of (*S*)-4-hydroxy-4'-(2-methylbutyloxycarbonyl)azobenzene (4 g, 0.01175 mol), potassium carbonate (8.1 g, 0.058 mol) and butanone (60 ml) in a nitrogen atmosphere. The mixture was heated under reflux for 48 hours. On cooling the solution was filtered and the solvent removed under reduced pressure. The residue was purified by column chromatography (silica gel stationary phase) using toluene: ethyl acetate (1:1) as eluent. This gave the product as an orange solid. It had m.p. 73.5-74.5 °C. Yield = 2.3 g, 0.005 mol, (47.2%), CI m/z 452, 451, 450 (M+1), $[\alpha]^{25}_{D}$ +4.2° (1.0 mol l^{-1}).

^{1}H NMR ($CDCl_3$): δ / ppm 0.9-0.98 (d, 3H, CH_2-$C\underline{H}_3$), 0.99-1.01 (t, 3H, CH-$C\underline{H}_3$), 1.22-1.4 (m, 12H, $(C\underline{H}_2)_6$), 1.42-1.48 ($C\underline{H}_2$-CH_3), 1.6-1.9 (m, 3H, C$\underline{H}$-CH_3 + CH_2=CH-$C\underline{H}_2$), 4.0-4.1 (t, $C\underline{H}_2$OAr), 4.1-4.3 (m, 2H, -$CO_2C\underline{H}_2$), 4.9-5.1 (t, 2H, $C\underline{H}_2$=CH), 5.7-5.9 (q, 1H, CH_2=C$\underline{H}$), 7.0 (d, 2H, aromatics), 7.8-8.0 (dd, 4H, aromatics), 8.1-8.3 (d, 2H, aromatics). IR υ / cm^{-1} : 1730 (C=O, ester), 1640, (vinyl), 1460 and 1400 (N=N), 1260 (CO_2CH_2).

Elemental analysis: Calc. C-74.6, H-8.5, N-6.2, found C-74.6 H-8.6, N-6.05.

1.5 (*S*)-4-(10-Pentamethydisiloxydecyloxy)-4'-(2-methylbutyloxycarbonyl)azobenzene (C_{10}Azo*B)

The appropriate vinyl mesogen (2 g, 0.0044 mol) and the catalyst, platinum divinyltetramethyldisiloxane complex were dissolved in dry toluene such that a Pt: alkene ratio in the range 1:10^3-10^6 mol was obtained. The solution was stirred under a nitrogen atmosphere and heated to 60°C then a solution of pentamethylhydrodisiloxane (0.196 g, 6.7 mmol / Si-H) (10 mol-% excess) in dry toluene (10 ml) was added dropwise. The reaction mixture was heated for a further hour at 60 °C and then heated under reflux until the residual Si-H absorption in the infra-red spectrum (2180 cm^{-1}) has been reduced to a very low level, usually 24 hours. On cooling, the solvent was removed under reduced pressure. The crude product was purified by column chromatography (silica gel stationary phase) using toluene as eluent. The solvent was removed under reduced pressure, dried under vacuum for 24 hours at 40 °C. This gave the desired product as a viscous orange fluid. Yield = 1.28 g, 0.0021 mol (57%), CI m/z 600, 598 (M^+), $[\alpha]^{25}_{D}$ +5.7° (1.0 mol l^{-1}, $CHCl_3$).

Thermal transitions: K 31.6 °C S_A °C 48.0 °C I.

^{1}H NMR ($CDCl_3$): δ 0.05 (d, 15H, PMDS), 0.45 (m, 2H, PMDS-$C\underline{H}_2$), 0.9-1.0 (m, 3H, CH_2-$C\underline{H}_3$), 1.0-1.2 (d, 3H, CH-$C\underline{H}_3$), 1.42-1.60 (m, 14H, $(C\underline{H}_2)_7$), 1.5-1.6 (m, 2H, $C\underline{H}_2CH_2$PMDS), 1.7-1.9 (m, 1H, *C$\underline{H}$-CH_3), 4.0-4.05 (t, 2H, $C\underline{H}_2$-OAr), 4.12-4.24 (m, 2H, -$CO_2C\underline{H}_2$), 6.8-7.0 (d, 2H, aromatics), 7.86-7.95 (dd, 4H, aromatics), 8.12-8.18 (d, 2H, aromatics). IR υ / cm^{-1} : 1730 (C=O, ester), 1600, (aromatics), 1460 and 1400 (N=N), 1260 (CO_2CH_2), 1020 (Si-O), 800 ($Si(CH_3)_3$.

Elemental Analysis: Calc. C-66.2, H-9.1, N-4.70, found C-66.5, H-8.90, N-4.7.

1.6 Racemic 4-(10-pentamethydisiloxydecyloxy)-4'-(2-methylhexyloxycarbonyl)azobenzene ($C_{10}Azo^{(\pm)}B$)

Synthesis carried out as detailed in 1.5 but using racemic 4-(9-decenyloxy)-4'-(2-methylbutyloxycarbonyl)azobenzene. Yield = 1.52 g, 0.0025 mol, 66%, CI m/z 599, (M+1), 598 (M^+).

Thermal transitions: K 31.5 °C S_A 50.0 °C I.

^1H NMR ($CDCl_3$): δ 0.05 (d, 15H, PMDS), 0.45 (m, 2H, PMDS-C$\underline{H}_2$), 0.92-0.98 (m, 3H, CH_2-C$\underline{H}_3$), 1.0-1.12 (d, 3H, CH-C$\underline{H}_3$), 1.45-1.60 (m, 14H, (C$\underline{H}_2)_7$), 1.5-1.6 (m, 2H, C$\underline{H}_2$$CH_2$PMDS), 4.0-4.05 (t, 2H, C$\underline{H}_2$OAr), 4.10-4.24 (m, 2H, -CO_2C$\underline{H}_2$), 6.8-7.0 (d, 2H, aromatics), 7.85-7.95 (dd, 4H, aromatics), 8.10-8.20 (d, 2H, aromatics).

IR υ / cm^{-1} : 1730 (C=O, ester), 1600, (aromatics), 1460 and 1400 (N=N), 1260 (CO_2CH_2).

Elemental Analysis: Calc. C-66.3, H-8.90, N-4.70, found C-66.5, H-8.90, N-4.7.

Physical Characterisation

^1H NMR spectra were carried out using Varian Gemini 200 and Varian 500 spectrometers. Infra-red spectra were recorded using a Perkin-Elmer FT-IR 1710 instrument. The transition temperatures of the siloxane derivatives were measured by polarising optical microscopy using a Nikon L-Ke polarising microscope linked to a Mettler FP80 hot stage and Mettler FP80 temperature controller. Samples were prepared as both thin film preparations between untreated glass substrates and in specially prepared 3.5 μm spaced cells with rubbed antiparallel polyimide alignment layers. Differential scanning calorimetry was carried out under a dry nitrogen flow with a Perkin-Elmer DSC 7 linked to a data station at a heating and cooling rate of 10 °C/min. Samples of ≈ 5 mg were employed. The temperature scale was calibrated against the melting temperature of indium.

Mesomorphic Behaviour of the LMM Organosiloxanes

The phase types and sequences of the chiral and achiral LMM organosiloxanes were confirmed by optical microscopy and DSC. The chiral and racemic vinyl precursors (1.4 a and b) exhibit only melting transitions of 73.5-74.5 °C and 75.2-76.2 °C respectively and no mesomorphic behaviour is observed. However, attachment of the pentamethyldisiloxane unit onto the vinyl precursors (1.5 a and b) results in the formation of a single enantiotropic smectic A phase, characterised by the typical focal conic fan texture when cooling out of the isotropic. It is interesting to note that despite the branched aliphatic chains in the terminal alkyl chain which can often promote the formation of tilted smectic phases[14], only an orthogonal smectic A phase is observed.

However, the presence of the siloxane moiety once again promotes the formation of smectic rather than nematic mesophases.

Thermal analysis by DSC confirmed the optical observations. The results are summarised in Table I.

Table I Phase transition data from DSC and optical microscopy. Results taken on the cooling cycle.

Sample	K-S_A / °C	ΔH / Jg^{-1}	S_A-I / °C	ΔH / Jg^{-1}
$C_{10}Azo^*B$	31.6	22.75	49.9	6.2
$C_{10}Azo^{(\pm)}B$	31.5	21.05	48.05	8.4

Both samples exhibited a small degree amount of biphasic behaviour close to the smectic A-isotropic phase transition. This weak biphasic behaviour appears to be typical of these organosiloxane materials[9,11] and is not a reflection of sample purity. Thin layer chromatography produced a sharp single spot trace for each product. Other workers[15,16] have reported similar biphasic behaviour in chemically pure materials.

EXPERIMENTAL

In this present work, the host liquid crystal used is a single component room temperature S_C^* material denoted $C_{10}C^*B$ synthesised in this group. The mesomorphic and ferroelectric properties of this material have already been reported elsewhere[9]. The structure of $C_{10}C^*B$ was shown previously in Figure 3 together with its phase transition temperatures. The very similar structures of the photo-reactive azo component and the ferroelectric host ensured complete miscibility of $C_{10}Azo^{(\pm)}B$ in $C_{10}C^*B$. During physical characterisation samples were contained in glass cells of 3.5 μm thickness, with a 25 mm^2 area patterned with transparent ITO film to enable electric fields to be applied across the cell, and with the inner glass surfaces coated with a polyimide alignment layer. The UV illumination of samples was by a Hg-arc lamp with its output filtered to select light in the 300 to 400nm range with a maximum output at 350nm. The glass of the sample cell was essentially transparent over this range of wavelengths. The power density of the U.V. light at the sample cell was always <10mWcm^{-2}. It was confirmed that U.V. irradiation caused no temperature jumps in the irradiated samples that could account for the effects discussed herein. When not illuminating samples with UV light, cells were kept in darkness.

Measurement of the magnitude of sample P_s in the S_C^* phase was by the well known current pulse technique[17]. A triangular wave driving voltage induces the liquid crystal molecules to flip between their two switched states. There is a short flow of current, which is measured as a function of time, as each molecule's polarisation dipole vector reverses direction and the area under this current pulse is then calculated (by an on-line microcomputer in the present work) to yield the value of P_S.

RESULTS AND DISCUSSION

Material Characterisation

It had been hoped that samples of pure $C_{10}Azo^*B$ would show a ferroelectric $S_C{}^*$ phase, thereby enabling the optical manipulation of ferroelectricity to be studied in a pure azo organosiloxane system. This was unfortunately not the case and for this reason we have here used $C_{10}Azo^{(\pm)}B$ as a photoisomerising guest in the ferroelectric host $C_{10}C^*B$, chosen for its similar chemical structure to the guest azo molecule . We note however that the since the chiral $C_{10}Azo^*B$ molecule exhibits a S_A phase it will be possible to study photomechanical manipulation of *electroclinic* switching (rather than the ferroelectric effects discussed herein) and such studies are presently underway.

The variation of spontaneous polarisation (P_s) with reduced temperature for pure $C_{10}C^*B$ and for a $C_{10}C^*B$+ 25% (wt:wt) $C_{10}Azo^{(\pm)}B$ mixture is shown in Figure 5 below. The phase transition temperatures $S_C{}^*$- I for $C_{10}C^*B$ and the $C_{10}C^*B$+ 25% (wt:wt) $C_{10}Azo^{(\pm)}B$ mixture are 56.2 °C and 50.0 °C respectively. The addition of the $C_{10}Azo^{(\pm)}B$ to the host $C_{10}C^*B$ causes a reduction in the P_s the pure host of ~20nCcm^{-2} at room temperature.

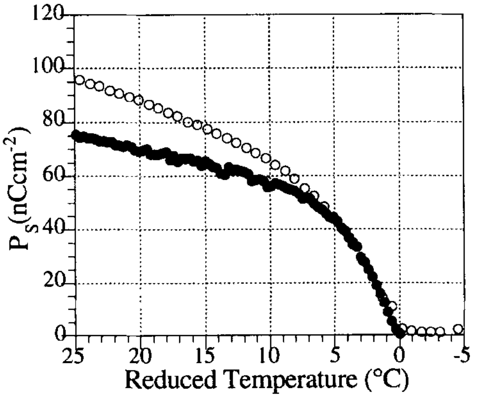

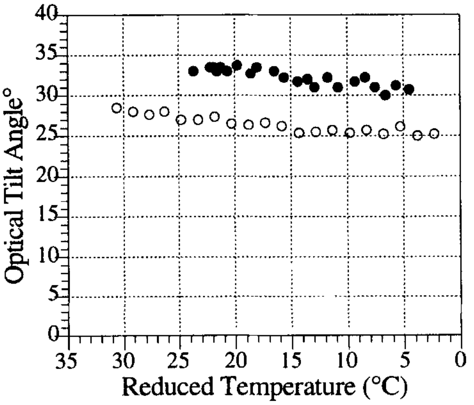

FIGURE 5 Showing the variation of spontaneous polarisation for pure $C_{10}C^*B$ (o) and $C_{10}C^*B$+ 25%(wt:wt) $C_{10}Azo^{(\pm)}B$ (•)

FIGURE 6 Showing variation of optical tilt angle for pure $C_{10}C^*B$ (o) and $C_{10}C^*B$+ 25%(wt:wt) $C_{10}Azo^{(\pm)}B$ (•)

However the resulting P_s of ~80nCcm^{-2} is still large fairly high for a low molar mass sample. Interestingly, the optical tilt angle (θ) of $C_{10}C^*B$ is increased by ≈ 25% upon addition of the azo racemate (Figure 6), but retains the property of being almost temperature independent, which is a highly desirable feature for device applications. The room temperature tilt angle of 33° is close to the 45° angle which is optimal for the construction of guest-host displays. We are currently carrying out further X-ray and dilatometry studies across the phase diagram to understand this unusual relationship between P_s and θ.

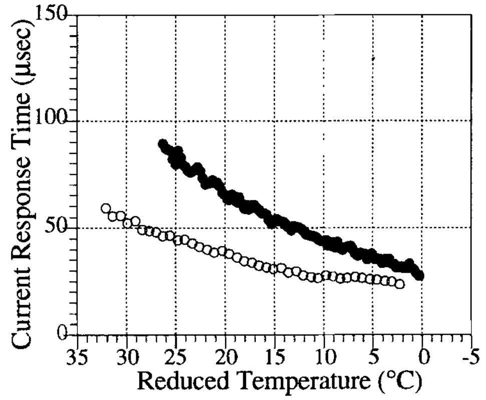

FIGURE 7 Showing the variation of current response time for pure $C_{10}C^*B$ (o) and $C_{10}C^*B$+25%(wt:wt) $C_{10}Azo^{(\pm)}B$ (•), 3.5µm thick sample switched by $60V_{rms}$ square-wave driving voltage.

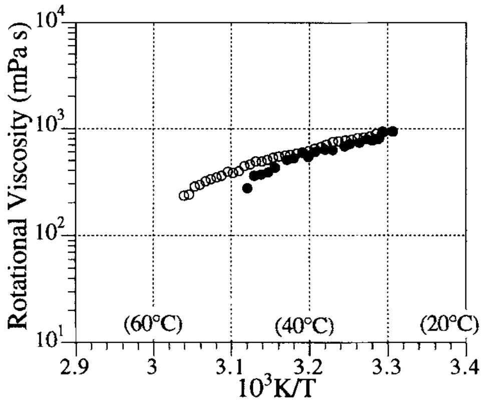

FIGURE 8 Arrhenius plot showing variation of rotational viscosity for pure $C_{10}C^*B$ (o) and $C_{10}C^*B$ +25%(wt:wt) $C_{10}Azo^{(\pm)}B$ (•)

The variation of response time of $C_{10}C^*B$ and the $C_{10}C^*B$+25% (wt:wt) $C_{10}Azo^{(\pm)}B$ is shown in Figure 7. The response time quoted is a *current response time*, defined as the time between the reversal in polarity of a square-wave switching voltage and the maximum point of the resulting current pulse as the sample's ferroelectric dipole reverses direction to align along the direction of the applied field. The more commonly quoted *optical response time*, a measure of the 10-90% rise-time in the optical transmission of a switching sample between crossed polarisers, cannot be used for materials with a tilt angle of >22.5°. If such a sample is rotated for optical extinction between crossed polarisers in one switched state, as the sample is switched to the second state the optical transmission will pass through a maximum before descending to the new stable value in the second switched state. A 10-90% optical rise-time is therefore not unambiguously defined, hence our adoption of a current-based technique. The relationship between the current response and optical response for a ferroelectric will in general be a complicated function. However we have found that for materials with tilt angles <22.5°, for which an optical response time can be measured, the current response time is only greater than the optical response by a multiplying factor of ≈ 1.2 and both show approximately the same temperature variation[18]. Thus except when the greater accuracy is required, the optical and the current response times can be regarded as essentially equal. The response time of both samples in Figure 6 compares very favourably at room temperature with commercially available multi-component mixtures optimised for display applications. This is noteworthy when one considers that $C_{10}C^{*}B$, for instance, is a pure material with no effort having gone into optimising its performance for display purposes.

From consideration of the shape of the current response of a ferroelectric liquid crystal it is possible, using the method of Escher et.al.[19], to calculate values for the rotational viscosity of molecules in the $S_C{}^{*}$ phase as they switch around a cone (Goldstone switching). These values are plotted in Figure 8 and indicate that the introduction of the azo dopant into pure $C_{10}C^{*}B$ only slightly reduces the magnitude of the rotational viscosity. The increase in current response time on addition of the organosiloxane dye is thus attributable essentially to the decrease in P_s and increase in θ for the mixture.

To summarise this section we may say that the addition of the guest dopant $C_{10}Azo^{(\pm)}B$ to $C_{10}C^{*}B$ has led to a useful room temperature ferroelectric material with low rotational viscosity, a moderately large P_s and large temperature independent tilt angle. These properties make it particularly useful for studying photomechanical processes. In the following section we shall explore the consequences of causing photoisomerisation of $C_{10}Azo^{(\pm)}B$.

Photoisomerisation of $C_{10}Azo^{(\pm)}B$

The presence of a reversible *trans/cis* isomerisation (c.f. Figure 1) for $C_{10}Azo^{(\pm)}B$ was confirmed through observation of changes in the absorption spectrum of the material dissolved in toluene. An absorption peak was present at 360nm, corresponding to the *trans* isomer, and a peak at 420nm corresponding to the *cis* isomer. When a sample of $C_{10}Azo^{(\pm)}B$ held in toluene is illuminated with UV light (360nm) then the peak corresponding to the *trans* isomers is found to decrease in height whilst the peak corresponding to the *cis* isomers increases. If scattering is neglected, the height of an absorbance peak is directly proportional to the concentration of the absorbing species (the well known Beer-Lambert law) and hence changes in the magnitude of an absorption peak can be directly related to changes that occur in the population of the absorbing species. Figure 9 shows the temporal variation of the height of the 360nm absorption peak (∝ concentration of *trans* isomer) for a solution of $C_{10}Azo^{(\pm)}B$ in toluene following a 1 hour exposure of the solution to UV light at a power density of $10mWcm^{-2}$. The UV lamp was turned off at time=0 and the height of the absorption peak measured at 10 minute intervals with the sample held in darkness at room temperature.

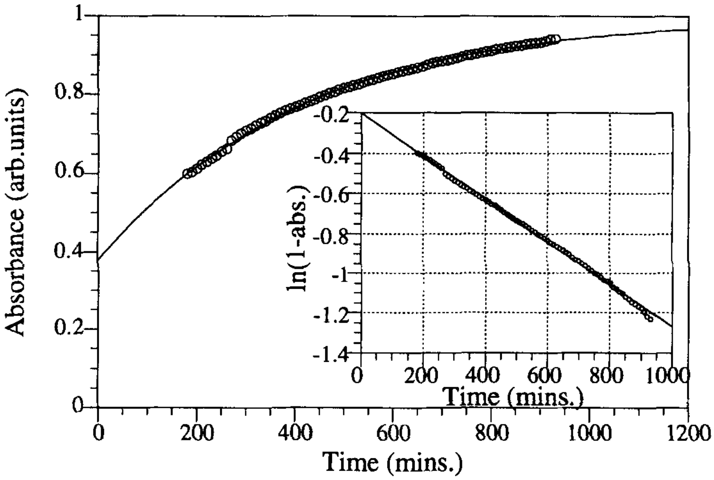

FIGURE 9 Temporal variation in height of 360nm absorption peak of $C_{10}Azo^{(\pm)}B$ in toluene following 1 hour exposure to UV light. Curve fits are from Eq. (3).

Basic physical chemistry enables us to draw some conclusions regarding the rate at which a simple reaction of the type ‘A→B’ occurs. (In the present instance we are interested in the *Cis→Trans* thermal relaxation of $C_{10}Azo^{(\pm)}B$). A *first order reaction* is defined[20] as one in which the rate of change of concentration of a species A with respect to time (t) is directly proportional to the concentration of A (denoted [A]). Hence for a first order reaction we have:

$$-\frac{d[A]}{dt} = k.[A] \tag{1}$$

where k is the *rate constant* for the reaction. For a reaction in which the total number of molecules per unit volume is a constant, it is a simple problem to solve Eq. (1) and show:

$$[\mathit{Trans}\ (t)] = [\mathit{Trans}\ (t \rightarrow \infty)] - C.\exp(-k.t) \tag{2}$$

Where C is a constant which will equal the concentration of *cis* isomers at t=0. From the discussion above, the concentration of *trans* isomers for $C_{10}Azo^{(\pm)}B$ is proportional to the magnitude of the 360nm absorption peak for the sample, whence:

$$\text{Absorbance (360nm)} = 1 - C'.\exp(-k.t) \qquad (3)$$

Where C' is a constant and the absorbance at large time has been normalised to unity. The data in Figure 9 has been fitted to Eq. (3). The inset confirms the excellent agreement between theory and experiment through a plot of ln(1-absorption) vs. time, which is predicted by Eq. (3) to be a straight line of gradient k. The rate constant k is found from this line fit as 1.1×10^{-3}/min. From Figure 9 we can conclude that the *cis/trans* thermal relaxation of $C_{10}Azo^{(\pm)}B$ in toluene is indeed a first order reaction.

Figure 10 shows the effect UV illumination on the P_s of a sample of $C_{10}C^*B$+25%(wt:wt) $C_{10}Azo^{(\pm)}B$ held at a temperature of 25°C. The sample is initially in darkness and has a P_s of $74nCcm^{-2}$ but after approximately 5 minutes a UV light is turned on and the P_s is seen to fall abruptly to $\sim29nCcm^{-2}$ and stabilise at this value for the duration of the UV exposure. The UV light is removed approximately 10 minutes afterwards, leaving the sample in darkness once more. The P_s is then seen to climb steadily back toward its original value of $74nCcm^{-2}$, over a period of ~400 minutes.

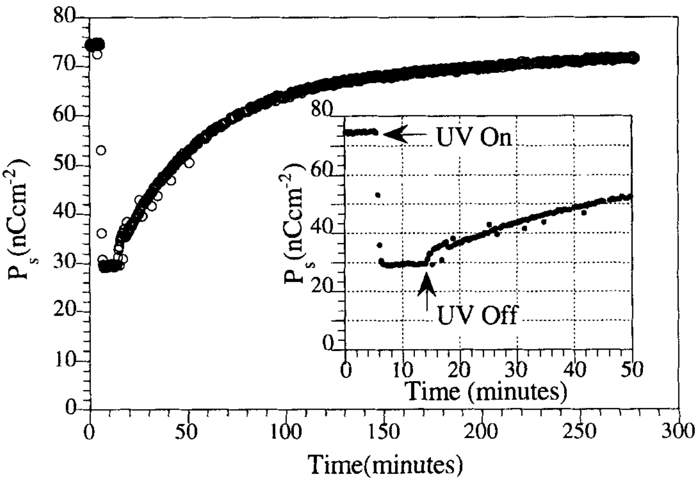

FIGURE 10 Showing the variation of P_S for a sample of $C_{10}C^*B$+25%(wt:wt) $C_{10}Azo^{(\pm)}B$ before during and after illumination with UV light.

The behaviour of the P_s in Figure 10 indicates that the UV illumination of $C_{10}C^*B$+25%(wt:wt) $C_{10}Azo^{(\pm)}B$ results in isomerisation of the azo guest molecules from their linear *trans* from to their bent *cis* state and this results in a disruption of the S_C* matrix and a consequent fall in the magnitude of P_s. Following removal of the UV light the *cis* molecules begin to relax to the thermally favoured *trans* state and the liquid crystal is able to return to its original ordered state. We note from Figure 10 however that the time taken for the P_s to return to within 10% of its original value (~400mins) is considerably shorter than the equivalent time taken for the relaxation of the absorbance of $C_{10}Azo^{(\pm)}B$ in toluene (~1000mins., c.f. Figure 9). Furthermore, if we make the assumption that the variation of the P_s of a sample is simply proportional to the number *cis* azo isomers tending to disrupt the $S_C{}^*$ matrix, then, from consideration of Eq. (2), we would assume that the variation of P_s with time would be of the form:

$$P_s(t) = P_s(t\to\infty) - P_s(t=0).\exp(-k't) \tag{4}$$

where k' is a constant. However, as can be clearly seen from Figure 11, an attempt to fit the variation of the P_s to Eq. (4) following removal of the UV light, fails (c.f. Figure 9 where the logarithmic inset-plot was linear).

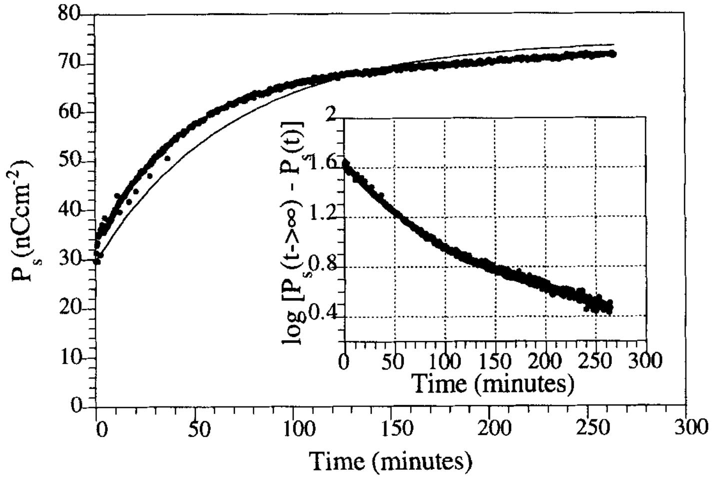

FIGURE 11 Showing the relaxation of P_s for $C_{10}C^*B$+25%(wt:wt) $C_{10}Azo^{(\pm)}B$ following the removal of UV illumination. The curve fit is to Eq. (4) and shows that the relaxation does not fit well to a single exponential (the inset graph would be linear if the fit were good c.f. Figure 9)

We must conclude from this data that the relaxation of P_s following UV isomerisation of a guest azo dye incorporated into the $S_C{}^*$ matrix is not governed simply by the first-order process that governs the *cis* to *trans* thermal relaxation of $C_{10}Azo^{(\pm)}B$ in an isotropic solvent.

The discrepancy between the rate and form of the relaxation of $C_{10}Azo^{(\pm)}B$ in toluene and the relaxation of the P_s of a sample of $C_{10}C^*B$+25%(wt:wt) $C_{10}Azo^{(\pm)}B$

following UV illumination may come about through a combination of several phenomena. Firstly, the *cis* to *trans relaxation* rate of $C_{10}Azo^{(\pm)}B$ measured in an isotropic solvent (toluene) will almost certainly change when the azo molecules are placed in the smectic matrix of $C_{10}C^{*}B$. We have attempted to determine the rate constant for the *cis/trans* relaxation for $C_{10}Azo^{(\pm)}B$ in $C_{10}C^{*}B$ by the same method as was used for the $C_{10}Azo^{(\pm)}B$/ toluene mixture (i.e. recording changes in absorption spectrum). However, for a liquid crystal sample, isomerisation of the azo guest molecules brings about a change in the *scattering* properties of the sample as the smectic matrix is disrupted. These changes in scattered light intensity are superimposed upon the changes which occur in the absorption spectrum of a sample and complicate the determination of rate constants. We have not yet been able to fully separate these contributions, but preliminary results suggest that the rate of the *cis* to *trans* relaxation for $C_{10}Azo^{(\pm)}B$ increases when it is incorporated into the $C_{10}C^{*}B$ host, bringing the overall relaxation times more into accord with the times associated with the relaxation of P_s following UV illumination of the sample. The increased relaxation rate for the $C_{10}Azo^{(\pm)}B$ molecules when dissolved in a liquid crystal, if confirmed, may be related to the extra energy it takes to isomerise an azo molecule to its bent *cis* state when it is confined in a liquid crystal matrix composed of linear $C_{10}C^{*}B$ molecules, rather than an isotropic solvent (toluene).

A second factor which may relate to the discrepancy between the predictions of Eq. (4) and the relaxation of P_s in Figure 11 are that extra rate determining processes are at work besides the *cis /trans* isomerisation. The rate at which the P_s relaxes will be linked to the rate at which the smectic layers of a sample can re-order themselves following their disruption by the bent guest *cis* isomers. Terms associated with molecular diffusion rates will therefore be important besides simply the isomerisation rate of the guest. One might therefore try to fit the data in Figure 11 to an equation. of the type of Eq. (4), but with extra exponential terms added to include diffusion processes. In the absence of a more quantitative understanding of the form of these extra terms, we not to performed such a fit, we are however investigating the possibility of light scattering experiments to learn more about the diffusion processes affecting the reordering of layers following isomerisation.

A third related factor will be the role of the tilt angle θ. Since this angle changes with concentration of azo moiety (c.f Figure 6) it would also be expected to change with concentration of *cis* species. P_S and θ do not appear to be simply related in these organosiloxane materials and therefore a further complex process related to the photoinduced changes in θ must convolute the temporal behaviour of P_S. We are currently examining this behaviour further.

CONCLUSION

We have reported the synthesis and characterisation of a new LMM photoisomerising organosiloxane ($C_{10}Azo^*B$) and its racemic analogue ($C_{10}Azo^{(\pm)}B$). These materials exhibit a single enantiotropic, room temperature S_A phase and an unusual polymeric siloxane/ mesogen/alkyl chain layer structure which confers ruggedness on the sample. A mixture of 25% (wt:wt) of $C_{10}Azo^{(\pm)}B$ with the room temperature ferroelectric organosiloxane $C_{10}C^*B$ (chosen for its similar chemical structure to the azo guest) has been characterised for tilt angle, spontaneous polarisation (P_s), response time and rotational viscosity. The mixture with a S_C^* phase from subzero to 50.0 °C shows a high (~35°), temperature independent tilt angle and a room temperature spontaneous polarisation of ~80nCcm^{-2}. The response time and rotational viscosity are comparable to values for commercial ferroelectric mixtures optimised for display usage.

The azo dyes are well known for their ability to undergo a reversible *trans/cis* isomerisation when illuminated with UV light. We have confirmed the presence of such an isomerisation for $C_{10}Azo^{(\pm)}B$ dissolved in toluene and shown the thermal *cis* to*trans* relaxation to be a first order reaction. In addition we have studied the consequences for the P_s of a sample of $C_{10}C^*B$+25%(wt:wt) $C_{10}Azo^{(\pm)}B$, of illumination with photoisomerising UV light. We have shown that the *cis* to *trans* isomerisation of the guest dye results in a fall in the P_s of a sample, which is reversible upon removal of the UV light. The results are in agreement with the hypothesis that the increased population of bent *cis* isomers occurring during UV illumination, tends to disrupt the ordering in the smectic host. The manner in which the P_s relaxes following removal of the UV light is broadly similar to the manner in which the population of *cis* isomers decays for $C_{10}Azo^{(\pm)}B$ in toluene however some differences are apparent, notably that the relaxation of P_s is more rapid. We have suggested mechanisms which may account for these differences.

ACKNOWLEDGEMENTS

We wish to thanks Dow Corning, Barry, U. K. for a major research grant that funded this research and provided a studentship for J.N.. H.G.W. thanks the SERC and Toshiba (Kawasaki) for a CASE studentship award.

REFERENCES

1. H. G. Walton, H. G. Coles, D. Guillon and G. Poeti, Liq. Cryst., In press (1994).
2. H. J. Coles, H. G. Walton, D. Guillon and G. Poeti, Liq. Cryst., 15, 4, 551 (1993).
3. H. G. Walton, and H. J. Coles, Ferroelectrics, *147*, 223, (1993).
4. C. H. Legge and G. R. Mitchell, J. Phys. D: Appl. Phys., 25, 492 (1992).

5. T. Ikeda, S. Kurihara, D. B. Karanjit and S. Tazuke, Macromolecules, 23, 3938 (1990).
6. H. J. Coles, H. Owen, J. Newton, P. Hodge, Liq. Cryst., 15, 5, 739, (1993).
7. R. B. Meyer, L. Liebert, L. Strzelecki, and P. Keller, 1975, J. Phys. Lett. (Paris), 36, L-69 (1975).
8 N. A. Clark and S. T. Lagerwall, Appl. Phys. Lett., 36(11), 899 (1980).
9. J. Newton, H. J. Coles, H. Owen and P. Hodge, Ferroelectrics, In press (1994).
10. M. Ibn-Elhaj, H. J. Coles, D. Guillon, A. Skoulios, J. Phys. II France, 3, 1807 (1993).
11. J. Newton, H. J. Coles, P. Hodge and J. Hannington, J. Mat. Chem., In press (1994).
12. S. T. Lagerwall, B. Otterholm and K. Skarp, Mol. Cryst. Liq. Cryst., 152, 503 (1987).
13. G. Poeti, E. Fanelli, L. Delamere, B. Heinrich, D. Guillon and A. Skoulios, Mol. Cryst. Liq. Cryst., 213, 145 (1992).
14. B. S. Furniss, A. J. Hannaford, P. W. G. Smith and A. R. Tatchell, in Vogel Textbook of Practical Organic Chemistry, Fifth Edition (Longmann, London, 1989), pp 78.
15. A. C. Griffin, S. R. Vaidya, R. S. L. Hung and S. Gorman, Mol. Cryst. Liq. Cryst. Lett., 1(5), 131 (1985).
16. A. Blumstein and O. Thomas, Macromolecules, 15, 1264 (1982).
17. K. Miyasto, S. Abe, H. Takezoe, A. Fukuda and E. Kuze, J. Appl. Phys. 22, L661(1983).
18. H. G. Walton, PhD. Thesis , University of Manchester (1994).
19. C. Escher, T. Geelhar, E. Böhm, Liq. Cryst. 3, 469, (1988).
20. Sienko and Plane, Chemical Principles and Properties, Second Edition (M^{c}Graw-Hill Kogakusha 1974). Chapter 5.